

Exciton Binding Energy Dependence of Hydrostatic Pressure and Temperature Inside a Cylindrical Quantum Dot

Nagwa Elmeshad, Hazem Abdelhamid, Hekmat Hassanein,
Safwan Abdelmola, and Sawsan Said

National Research Center, Cairo, Egypt
(Received June 2, 2008)

We studied the effects of the hydrostatic pressure and the temperature on the exciton binding energy confined inside a cylindrical GaAs quantum dot. The exciton binding energies are obtained by a variational approach. We solved the Schrödinger equation via the proper choice of the exciton trial wave function. The behavior of the exciton binding energy was examined at different pressure and temperature values for different quantum dot sizes. The present study shows an increase of the exciton binding energy as the hydrostatic pressure increases, and, in contrast, it decreases when the temperature is raised.

PACS numbers: 73.21.La

I. INTRODUCTION

The techniques of molecular-beam epitaxy (MBE) and metal-organic chemical-vapor deposition (MOCVD) have been used to grow high-quality hetero-junctions; thus the growth of systems consisting of alternate layers of two different semiconductors with controllable thickness has become possible. These hetero-structures have stimulated new works in semiconductor physics over the past years. For example, we are now able to control layers so thin that some of the quantum confinement effects of electrons and holes can readily be seen. For example, in bulk GaAs, the exciton resonances are very weak and thus can be observed only at very low temperatures. However, in nano-structures, the exciton resonances become considerably sharper due to the quantum-confinement effect, and thus can be observed easily at room temperature. In recent years, the exciton problems in semiconductor nano-structures have been studied extensively [1-5].

The formation of self-assembled quantum dots (SAQDs) in different material systems such as GaAs/AlGaAs or GaInAs/AlGaAs hetero-structures has been demonstrated successfully [6]. The stopping of the growth process in the initial state of formation of the nano-structures results in QDs free of defects and dislocations. Adler *et al.* [7] have observed optical transitions from higher energetic dot levels in the photoluminescence (PL) spectra at different excitation levels in InAs/GaAs SAQDs. Their observed PL lines are in good agreement with the calculated transitions between the eigenstates obtained by solving the effective-mass Schrödinger equation in cylindrical coordinates. Additionally, in their very simple model, they have found only one quantized electronic level in the QD. Strain modifies the band structure via the deformation potentials, and the shift of the conduction band

is proportional to the hydrostatic strain [8]. A study of the temperature dependence of the PL emission from InAs QDs in a strained $\text{Ga}_{0.85}\text{In}_{0.15}\text{As}$ QW has shown [9] that the energy shift with the temperature generally follows the InAs band gap variation for temperatures up to about 200 K, and that when the temperature is further raised the QD peak red shifts faster than the InAs gap variation. An understanding of the pressure and temperature dependence of QD emissions may be very important for building efficient lasers.

It is well established that the confinement of excitons in semiconductor nanostructures yields an enhanced excitonic effect, which can be exploited in the design of novel optoelectronic devices. The exciton binding energy increases with the spatial confinement reaching a peak at some critical confinement width (which depends on the potential barrier height). This implies the existence of a critical confinement limit where the quantum confinement effect is a maximum. There has been growing interest in the topic regarding the confined exciton states in various nanostructures [10–12]. A reason for this interest is the possible simplification of the intensive computation involved in obtaining exciton binding energies in quantum structures such as QDs systems. Thus, a large binding energy allows excitons to become stable, and it is favorable for the room temperature operation of devices based on excitons. Therefore a proper understanding of the temperature effect on the excitons in these confined systems is necessary for the correct interpretation of the optical data. Besides, there has been growing interest in the topic regarding the confined exciton even at room temperature [13, 14].

El Moussaouy *et al.* [15, 16] published two articles, one [15] regarding the hydrostatic stress dependence of the exciton-phonon coupled states in a cylindrical GaAs QD. But going through their model we noticed two different issues between their theoretical model and the present model. The first issue concerns their trial wave function, which is different from ours. The second issue is that they considered an infinite confinement in the in-plane direction. The second [16] article concerns the thermal effect on bound excitons in a CdTe/ $\text{Cd}_{1-x}\text{Zn}_x\text{Te}$ cylindrical QD. Therefore in our present work we will study the hydrostatic pressure and temperature effects on bound excitons in a GaAs/ $\text{Al}_x\text{Ga}_{1-x}\text{As}$ cylindrical QD with a finite confinement potential induced by the barrier material. This paper is organized as follows: in Section 2 we show our theoretical model, the results and discussion are given in Section 3, and finally in Section 4 we present our conclusions.

II. THEORETICAL MODEL

The Hamiltonian for an exciton confined inside a cylindrical QD of radius R and height L in the effective mass and non-degenerated band approximations can be presented

as

$$\begin{aligned}
H = & -\frac{\hbar^2}{2m_e^*} \left[\frac{\partial^2}{\partial r_e^2} - \frac{1}{r_e} \frac{\partial}{\partial r_e} + \frac{r_e^2 - r_h^2 + r^2}{r_e r} \frac{\partial^2}{\partial r_e \partial r} \right] \\
& -\frac{\hbar^2}{2m_h^*} \left[\frac{\partial^2}{\partial r_h^2} - \frac{1}{r_h} \frac{\partial}{\partial r_h} + \frac{r_h^2 - r_e^2 + r^2}{r_h r} \frac{\partial^2}{\partial r_h \partial r} \right] \\
& -\frac{\hbar^2}{2\mu} \left[\frac{\partial^2}{\partial r^2} + \frac{1}{r} \frac{\partial}{\partial r} \right] - \frac{\hbar^2}{2m_e^*} \frac{\partial^2}{\partial z_e^2} - \frac{\hbar^2}{2m_h^*} \frac{\partial^2}{\partial z_h^2} \\
& + V_e(r_e, z_e) + V_h(r_h, z_h) + \frac{e^2}{\epsilon} \left[-\frac{1}{\sqrt{r^2 + (z_e - z_h)^2}} \right].
\end{aligned} \tag{1}$$

where the relative coordinate $r = |\vec{r}_e - \vec{r}_h|$, and the exciton reduced mass $\mu = \frac{m_e^* m_h^*}{m_e^* + m_h^*}$.

II-1. Hydrostatic pressure

Applying pressure along the growth axis (z-direction), the electron effective mass inside the QD and inside the barrier changes with the pressure as $m_e^*(p) = m_o(0.0665 + 0.00055p)$, and the effective mass of the hole becomes $m_h^* = m_o(0.087 + 0.00064p)$, where p is the pressure value [17, 18]. The total band gap difference between GaAs and $\text{Ga}_{1-x}\text{Al}_x$ As as a function of x (Al concentration) and the pressure p is given by $\Delta E_g(x, p) = \Delta E_g(x) + pD(x)$, where $\Delta E_g(x) = 1.247x$ eV and $D(x)$ is the pressure coefficient of the band gap given by $D(x) = (-1.3 \times 10^{-3})x$ eV/kbar [19, 20]. Assuming the conduction band offset parameters for electron and hole are 65% and 35%, respectively. The confinement potential as a function of the pressure is given as follows:

$$\begin{aligned}
V_i = V_i & \quad 0 & \text{if } r \leq R, |Z| \leq L(p)/2, \\
V_i(p) & \quad & \text{if } r > R, |Z| \leq L(p)/2, \\
& \quad & \text{otherwise,}
\end{aligned}$$

where $i = (e, h)$, V_e and $V_e(p)$ are defined as $V_e = 0.65\Delta E_g(x, 0)$, and $V_e(p) = 0.65\Delta E_g(x, p)$, similarly the hole confinement potential is considered as $V_h = 0.35\Delta E_g(x, 0)$ and $V_h(p) = 0.35\Delta E_g(x, p)$. The dielectric constant is represented by $\epsilon(P) = 13.1 - 0.0088P$. The variation of the QD height with the pressure is given by [21] $L(p) = L[1 - (s_{11} + 2s_{12})p]$, where $s_{11} = 1.16 \times 10^{-3} \text{ kbar}^{-1}$ and $s_{12} = -3.7 \times 10^{-4} \text{ kbar}^{-1}$ are the elastic constants of the GaAs material and L is the original height of the QD.

In order to determine the exciton binding energy, we choose the following trial wave function:

$$\psi_{exc} = F_e(r_e, z_e, p) F_h(r_h, z_h, p) \exp\{-\alpha \sqrt{(r_e - r_h)^2 + (z_e - z_h)^2}\}, \tag{3}$$

with $F_i = f_i(r_i)g_i(z_i, p)$, where f_i and g_i are the single particle (electron and hole) wave functions in the in-plane and z-direction, respectively:

$$f_i(r_i) = \begin{cases} J_0(\theta r) & \text{for } r \leq R, \\ BK_0(\beta r) & \text{for } r > R, \end{cases}$$

$$g_i(z_i, p) = \begin{cases} \cos(M(p)z) & \text{for } |Z| \leq L(p)/2 \\ A \exp(-q(p)|z|) & \text{for } |Z| > L(p)/2 \end{cases}$$

Here J_0 , K_0 are the modified Bessel functions of zero order. α is the variation parameter. The ground-state energy of the exciton under the pressure effect is calculated as follows:

$$E_{exc}(p) = \min_{\alpha} \frac{\langle \psi_{exc} | H | \psi_{exc} \rangle}{\langle \psi_{exc} | \psi_{exc} \rangle},$$

and the exciton binding energy is obtained by the relation

$$E_b(p) = E_e(p) + E_h(p) - E_{exc}(p),$$

where $E_e(p)$ and $E_h(p)$ are the single particle ground-state energies (eigenvalues of F_i).

II-2. Temperature effect

Monomer *et al.* [22] showed that for the Γ_1 and X_1 minima the temperature coefficients of the minima are a good approximation independent of the aluminum concentration, hence the barrier potential can be obtained using $V_e=0.65\Delta E_g(x)$, $V_h=0.35\Delta E_g(x)$, where $\Delta E_g(x)=E_{gGaAlAs}(x, T) - E_{gGaAs}(x, T)=1.115x+0.37x^2$. We used the following relations to calculate the electron and hole effective masses and the dielectric constant, respectively [23]:

$$m_e^* = \frac{m_o}{1 + 7.51((2/E_g) + (E_g + 0.34)^{-1})},$$

$$m_h^* = \frac{E_g m_o}{(20 - E_g)}, \quad \text{and} \quad (T) = 12.4(1 + 1.2(10^{-4}T)).$$

Here E_g is the GaAs direct energy gap and is given by the Varshni formula [23]:

$$E_{gGaAs}(T) = 1.519 - \frac{5.405 \times 10^{-4}T^2}{(T + 204)}.$$

III. RESULTS AND DISCUSSIONS

In order to illustrate the pressure effect on the exciton binding energy, we consider a cylindrical QD made of GaAs embedded in $Al_xGa_{1-x}As$ material. The physical parameters corresponding to GaAs are: $\varepsilon=(P)=13.1-0.0088P$, the exciton effective Bohr radius at zero pressure is $a_{exc}^*=183.8 \text{ \AA}$. Figure 1(a) and 1(b) show the variation of the exciton binding energy as a function of the half width ($L/2$) at a constant radius $R = 15 \text{ nm}$, and as a function of the radius R at constant half width $L/2 = 7 \text{ nm}$, respectively. The three curves in each figure are calculated at three different values of the applied hydrostatic pressure along the z -direction, $p = 0, 10, \text{ and } 40 \text{ kbar}$. The binding energy as the radius or the half width reduces, reaches a maximum, and then decreases, which is qualitatively similar to our previous results [13] for the exciton state without applying pressure. At small R values, discrete exciton levels are absent in the well, and the exciton's particle wave functions are

distributed outside the cylinder. When increasing the cylinder radius R , the exciton energy levels fall from the continuum spectrum into the well. By looking at Figure 1(b) we observe that the exciton binding energy decreases faster when the radius increases than when the half width increases Figure 1(a).

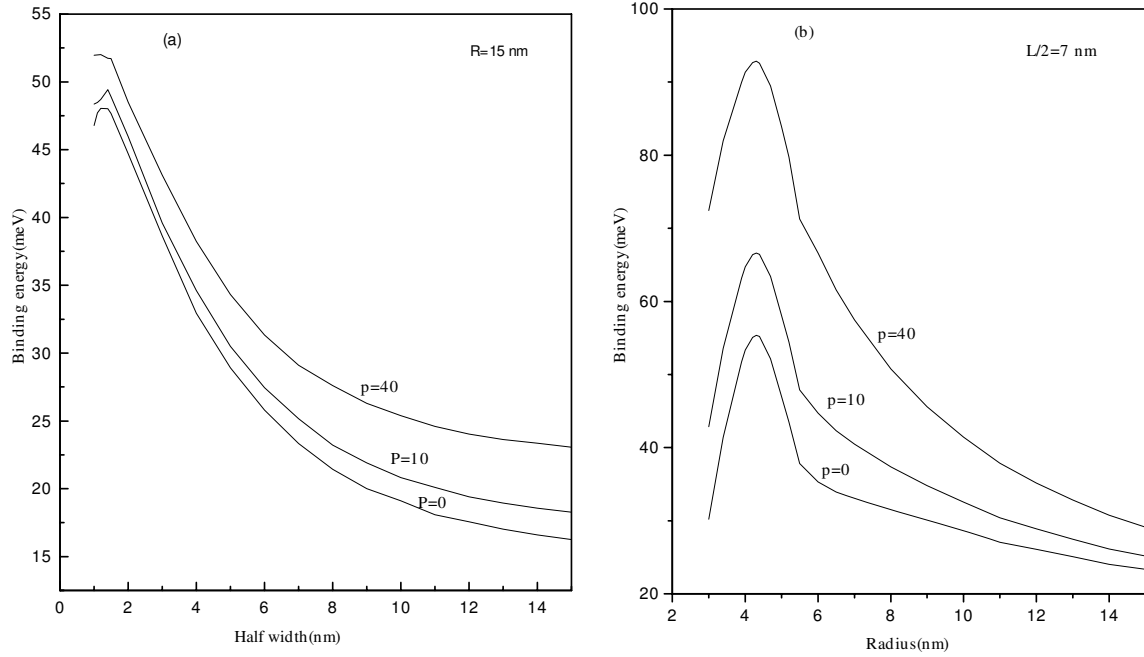


FIG. 1: (a) The exciton binding energy as a function of the half width at three different values of the pressure, at $R = 15$ nm. (b) Exciton binding energy as a function of the radius R at three values of pressure, $L/2 = 7$ nm.

The hydrostatic pressure increases the exciton binding energy, meaning that the exciton state will be more stable inside the QD under pressure than in a QD without pressure if its radius is within the range 6 to 8 nm.

In Figure 2(a) and 2(b) we display the variation of the exciton binding energy with the applied pressure at different half widths ($L/2 = 2, 5,$ and 10 nm at $R = 10$ nm) and different radii [$R = 5, 10$ and 20 nm at $L/2 = 9$ nm], respectively. The increase of the three curves' slope is a more noticeable value with an increasing R than when increasing the QD half width, that is, again as we said before, the exciton state becomes more stable in the presence of the applied pressure. Thus we obtained the sudden decrease of the exciton binding energy in the in-plane of the QD, which is not the situation in the z -axis (L -direction) Figure 1(a).

To study the effect of the barrier height on the exciton binding energy at high temperature, we present Figure 3. Figures 3(a) and 3(b) show the variation of the exciton binding energy with the QD radius R at $L/2 = 7$ nm, when the temperature is zero and 300 K at two different values of Al concentration $x = 0.4$ and 0.2 , respectively. Here we

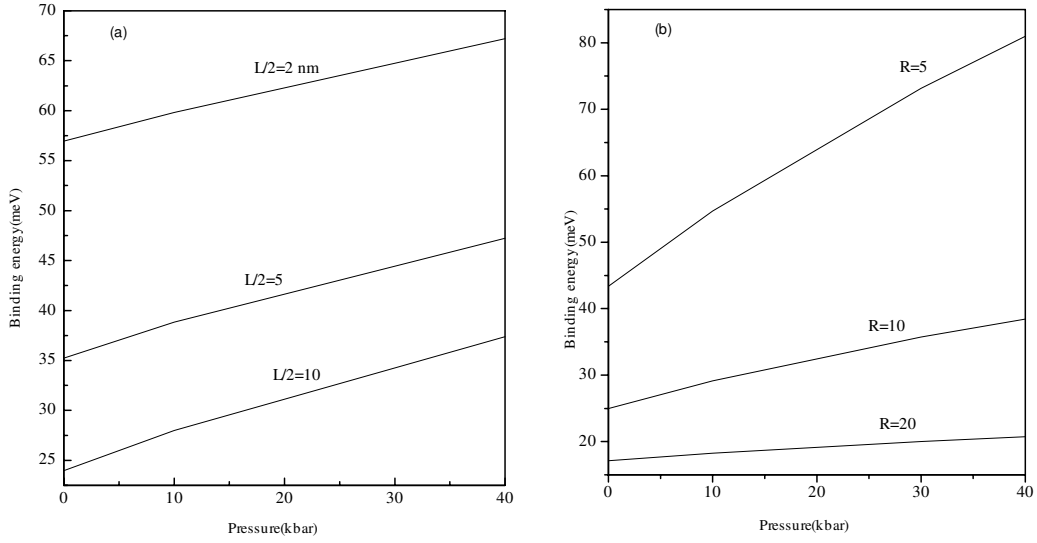


FIG. 2: The exciton binding energy versus the pressure for three different values of $L/2$, at $R = 10$ nm. (b) Exciton binding energy versus the pressure for three different values of R , at $L/2 = 9$ nm.

note that the temperature effect on the exciton binding energy is qualitatively similar to the pressure effect. We see that the exciton binding energy decreases with a raise in the temperature, in contrast with the hydrostatic pressure effect. Looking at Figures 3(a) and 3(b), we can say that the higher the binding energy the higher the x value and the lower the temperature values.

Figure 4(a) and 4(b) display the variation of the binding energy with the temperature at three different values of the QD half width ($L/2 = 5, 8,$ and 10 nm) and at three different radii $\{R = 7, 10,$ and $15\}$, respectively. Comparing the slopes of the curves in Figure 3 and Figure (2), we may say that the increase of the slopes of the plots in Figure (2) is more noticeable than that of Figure 3. In other words the hydrostatic pressure raises the exciton binding energy, and consequently we get a stable excitonic state. This increase of the exciton binding energy is quite noticeable when compared to its decreasing at high temperature.

Our results are in qualitative agreement with the results in Ref. [15, 16]. Finally, we give a comparison between our results and the Ref. [15] results, even though those authors showed that the exciton-phonon coupled states in their Hamiltonian increases the exciton binding energy. However, here we choose a different trial wave function (no separation of the exciton motion in the $x - y$ plane from the z -direction), and without including exciton-phonon coupling, we obtained a higher value for the exciton binding energy than in Ref. [15], because we considered a finite confinement potential in the $x - y$ plane.

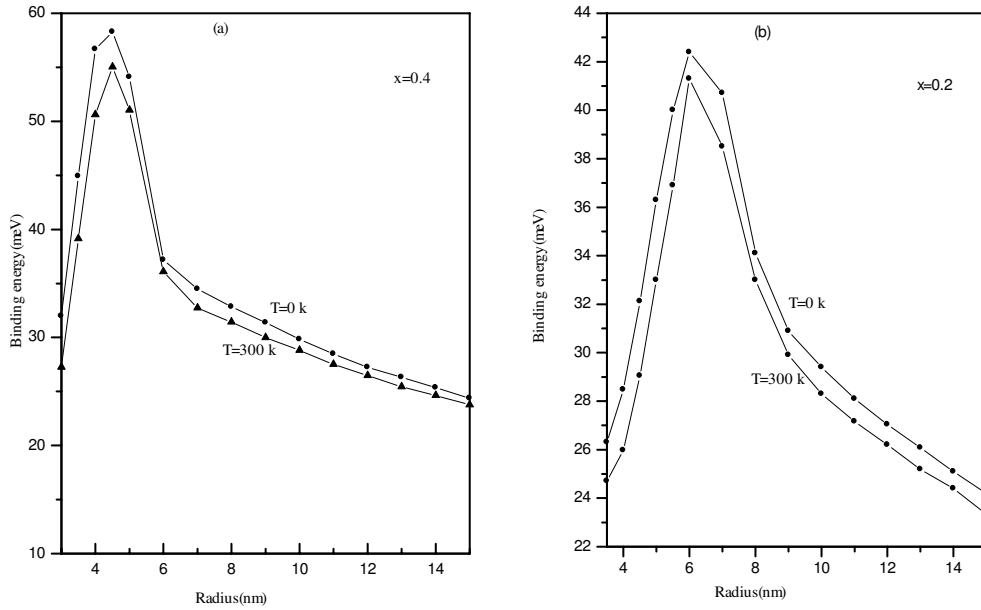


FIG. 3: (a) Variation of exciton binding energy as a function of the Radius at $L/2 = 7$ nm, $T = 0$, 300 K and $x = 0.4$. (b) The same but at $x = 0.2$.

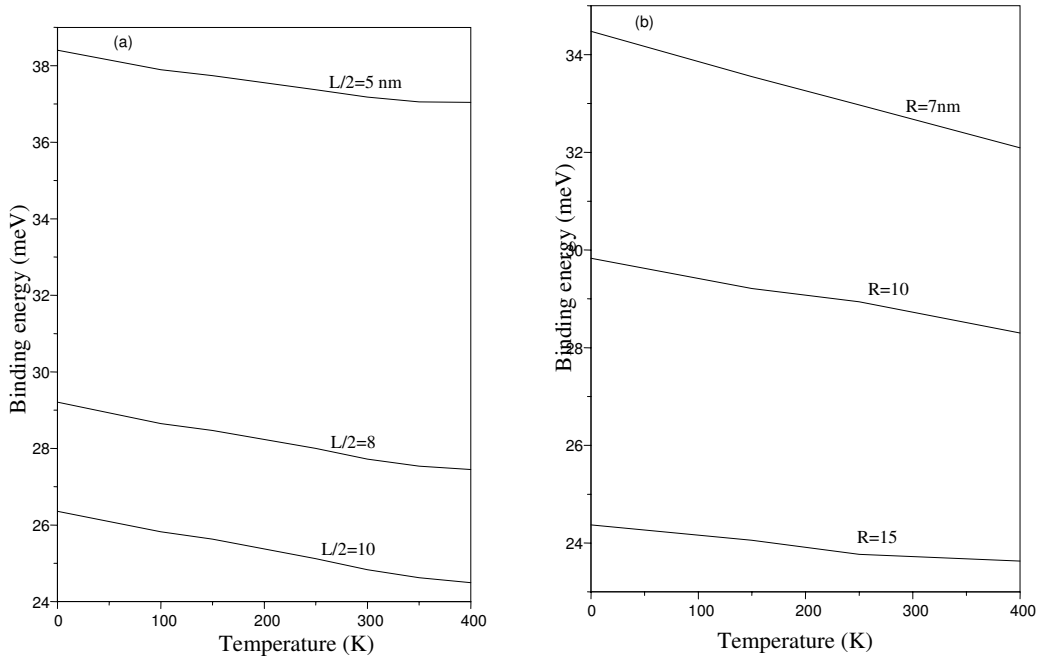


FIG. 4: (a) Exciton binding energy versus temperature for $R=9$ nm at $L/2 = 5, 8$ and 10 . (b) Variation of binding energy with temperature for $L/2 = 7$ nm at $R = 7, 10$, and 15 nm.

IV. CONCLUSIONS

We solved the Schrödinger equation variationally for excitons confined inside a cylindrical QD manufactured from GaAs and embedded in $\text{Al}_x\text{Ga}_{1-x}\text{As}$ as a barrier material. We choose a trial wave function with one variational parameter. The hydrostatic pressure effect on the exciton binding energy was examined by applying hydrostatic pressure along the QD growth axis (z -axis). We obtained higher values for the binding energy than those found in Ref. [15]. We obtained an increase of the exciton binding energy due to the presence of the hydrostatic pressure, and thus the excitonic state becomes more stable. In contrast the exciton binding energy decreases at high temperatures. The present work could be helpful for a correct interpretation of the optical data of QDs and for the designers of devices based on excitons.

References

- [1] K. J. Moore, G. Duggan, K. Woodbridge, and C. Roberts, Phys. Rev. B **41**, 1090 (1990); **41**, 1095 (1990).
- [2] M. M. Dignam and J. E. Sipe, Phys. Rev. B **41**, 2865 (1990).
- [3] P. Bigenwald, B. Gil, A. Kavokin, and P. Christol, Phys. Stat. Sol. A **183**, 125 (2001).
- [4] P. F. Gomes *et al.*, Phys. Stat. Sol. c4, No. 2, 385 (2007).
- [5] N. Kotera *et al.*, Microelectronic Engineering **63**, 301 (2002).
- [6] K. Watanabe, N. Koguchi, and Y. Gotoh, Jpn. J. Appl. Phys. **39**, L79 (2000).
- [7] F. Adler *et al.*, J. Appl. Phys. **80**, 4019 (1996).
- [8] M. P. C. M. Krijin, Semicond. Sci. Technol. **6**, 27(1991).
- [9] D. P. Popescu, P. G. Eliseev, A. Stintz, and K. J. Malloy, Semocond. Sci. Technol. **19** 33 (2004).
- [10] C. C. Yang, L. C. Liu, and S. H. Chang, Phys. Rev. B **58**, 1954 (1998).
- [11] K. L. Janssens, F. M. Peeters, and V. A. Schweigert, Phys. Rev. B **63**, 205311 (2001).
- [12] M. Brasken, M. Lindberg, D. Sundholm, and J. Olsen, Phys. Rev. B **61**, 7652 (2000).
- [13] M. Bayer and A. Forchel, Phys. Rev. B **65**, 041301 (2002).
- [14] S. A. Safwan, M. H. Hekmat, N. A. El-Meshad, Fizika A **15**, 1 (2007).
- [15] A. El Moussaouy, D. Bria, and A. Nougouai, Physica B, Cond. Matt. **370**, 178 (2005).
- [16] A. El Moussaouy, D. Bria, and A. Nougouai, Solar Energy Materials & Solar Cells **90**, 1403 (2006).
- [17] B. Sukumar and K. Navaneethkrishnan, Phys. Stat. Sol. b **158**, 193 (1990).
- [18] K. Reimann, M. Holtz, K. Syassen, Y. C. Lu, and E. Bauser, Phys. Rev. B **44**, 2985 (1991).
- [19] S. Adachi, J. Appl. Phys. **58**, R1 (1985).
- [20] T. S. Koh, Y.-p. Feng, X. Xu, and H. N. Spector, J. Phys: Condens. Matter **13**, 1485 (2001).
- [21] H. O. Oyoko, C. A. Duque, and N. Porrás-Montenegro, J. Appl. Phys. **90** (2001) 819.
- [22] B. Monomar, K. K. Shih, and G. D. Pettit, J. Appl. Phys. **47**, 2604 (1969).
- [23] J. S. Blakemore, J. Appl. Phys. **53**, R123 (1982).
- [24] M. Elabsy, Egypt. J. Sol. **23**, 267 (2000).